Comparison of the far wake behind dual rotor and dual disk configurations

Okulov, Valery; Mikkelsen, Robert Flemming; Naumov, I. V.; Litvinov, I. V.; Gesheva, E.; Sørensen, Jens Nørkær

Published in:
Journal of Physics: Conference Series (Online)

Link to article, DOI:
10.1088/1742-6596/753/3/032060

Publication date:
2016

Document Version
Publisher's PDF, also known as Version of record

Comparison of the far wake behind dual rotor and dual disk configurations

2016 J. Phys.: Conf. Ser. 753 032060

(http://iopscience.iop.org/1742-6596/753/3/032060)

Comparison of the far wake behind dual rotor and dual disk configurations

V L Okulov [1,2], **R F Mikkelsen**[1], **I V Naumov**[2], **I V Litvinov**[2], **E Gesheva**[2], **J N Sørensen**[1]

[1]Department of Wind Energy, Technical University of Denmark, Lyngby, Denmark
[2] Kutateladze Institute of Thermophysics SB RAS, Novosibirsk, Russia

E-mail: vaok@dtu.dk

Abstract. There is an increasing interest in studying the development of far wakes behind two or more interacting wind turbines in order to determine the influence of wake interaction in relation to the design of wind farms. The focus of this experimental study is to understand and describe the resulting wake features for two rotors subjected to different operating and spatial conditions. As a part of this, a comparison with the wake development behind two disks replacing the rotor models was performed to determine the difference between the two wake systems.

LDA and Stereo PIV experiments were carried out to study the development of far wakes behind configurations of dual HAWT wind turbine rotors and dual circular disks. The setups were placed in the middle of a water flume. The initial flow in the flume is subjected to a very low turbulence level, limiting the influence of all external disturbances in order to focus the study to the inherent wake instability.

As a result of the investigation, we obtained decays of profiles for the velocity deficit and turbulent pulsations in the far wakes behind both dual rotor and dual disk configurations. By using regression techniques to fit the obtained velocity profiles the experimental data were approximated by identical analytical models and compared to each other. An identical rational dependence with the same powers, but with different coefficients, was found for the two configurations.

1. Introduction

The velocity deficit and the turbulence level are the two main parameters defining the available power and structural stability of wind turbines located in the wake of other turbines in a wind farm. In spite of the extensive investigations of turbine interaction in wind farms, the prediction of the wake development and associated decay are still open questions [1,2].

In the present paper, we investigate the far wake behind two configurations consisting of two identical three-bladed models of HAWT rotors and of two equal solid disks, respectively. Both dual systems were studied at the same spatial positions in a uniform inflow (Fig. 1). The purpose of the analysis is to measure and reconstruct the wake development and decay behind the rotor-rotor and the disk-disk systems to describe the evolution of the wake profiles and their functional dependence, corresponding to the behavior found for wakes behind single rotors [3-5] or single disks [6]. In the mentioned articles, the development of the two far wakes was found to yield the same powers, but different coefficients. Both types of wake decay indicate quite different initial states, but very close nature of the attenuation constant with the same power rate. Moreover, identical attenuation functions

in the wake behind a single rotor were discovered for different operating regimes of tip speed ratios (TSR) greater than two [3]. Therefore, in the present study, special attention was paid to detect and categorize the various types of the attenuation constants for all decay wakes generated in the new setup configurations behind the two wind turbine rotors operating at TSRs from 2 to 8.

2. Experimental Method

The experiment is carried out in a water flume of length 35m, 3m width and an operative height of 0.9m. The 3m wide test section is fitted with transparent walls at a distance of 20 m from the channel inlet. The freestream flow speed in the flume was U = 0.54 m/s. The boundary layer thickness (≈ 0.2 m) and the level of turbulent pulsations (≈ 2 %) for the undisturbed flow in the test section were measured in previous experiments for a single wind turbine model [7-8]. The axis of setup with the rotors or disks was positioned at a height of 0.5m from the channel bottom and 1.5 m away from the two walls of the flume (Fig. 1).

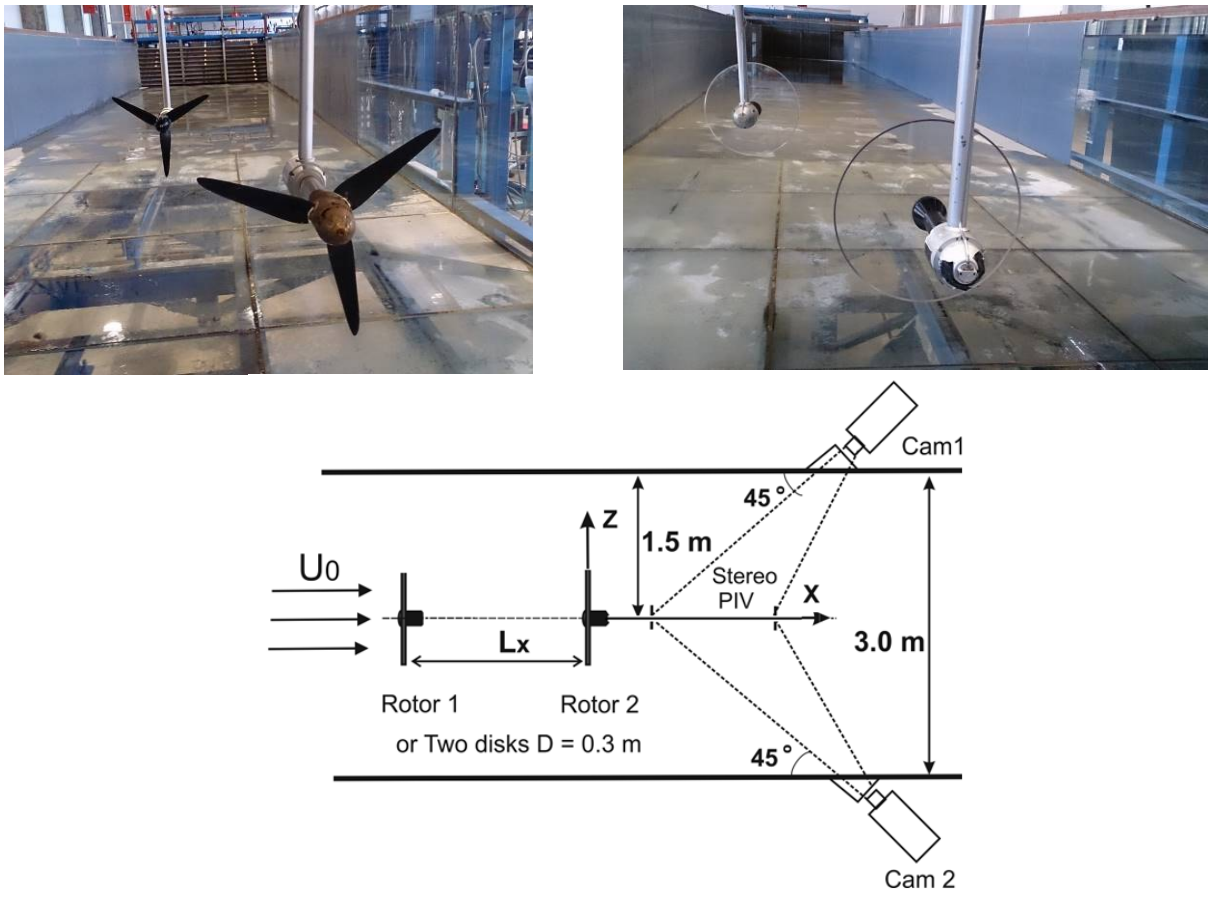

Figure 1. Photos and sketches of the experimental setup.

The two identical disks have a diameter D_d= 0.3 m and a thickness of 0.01 m and the two identical three-bladed rotors have a diameter D = 0.376 m and a blade length of 0.159 m. The spacing distance L_x was changed in the range 4D–8D.

Both rotors were designed by a combined blade element/lifting line (BE/LL) theory with a constant lift coefficient C_L= 0.8 for the airfoil sections SD7003 [9] and a Goldstein circulation distribution at an optimum tip speed ratio λ = 5 [10], where λ = ΩR/U_0, R – rotor radius, and Ω - the angular speed of the rotor. The rotors were driven independently by a servomotor, which was operated at a constant rotational speed within 2% accuracy. During the experiments, the tip speed ratios were varied from 3 to 9 for each rotor.

Stereo PIV experiments were carried out to study the far wake development, which was measured at different longitudinal sections downstream of the second rotor or disk at distances up to 40*D*. The features of the decaying wake past the bodies were determined using a Stereo-PIV equipment from Dantec. The characteristics of the equipment are described in [7]. The light source of the PIV light sheet was a Litron 200-15 PIV Nd:Yag pulse laser with the following characteristics: 200 mJ of pulse energy and an operational frequency of 10 Hz. The images were recorded with a CMOS Speedsence 1040 camera with a focal distance of 55 mm and 2320x1726 pixel resolution.

The interrogation area of the PIV measurements was divided into different windows with 50 mm overlapping, ensuring a consistent prediction of the velocity field in the entire area. The dimension of each of the windows of the PIV measurements was 732x430 mm. All measurement windows were positioned at the same place at the glass section of the test area, and the distance between the second rotor (or the disk) was changed by a stepping motion of the movable platform with the setups along the X-axis (Fig. 1). This step motion of the movable setup allowed us to carry out measurements in the next windows, keeping the optical system in the same immobile position for the light sheet and the camera. The final velocity field for every testing window was simulated by averaging 200 instantaneous PIV samples in the light sheet of the XY plane by Dynamic Studio software, which provided two components of the velocity field (*U, V*) in a vertical cross-section along the rotor or disk axis. The total velocity fields were glued together by combining all flow patterns of the measuring windows.

3. Results

Fig. 2 shows downstream variations of the maximum axial velocity deficit $\frac{\Delta U}{U_0} = \frac{U_0 - U}{U_0}$ in the wake behind the disk-disk setup (D-D) for the different distances, L_x= 4, 6, 8*D*. The experimental data using regression techniques to fit all velocity profiles were approximated by the rational function $G(x) = \Delta U(x)/U_0 = a(x - x_0)^{-2/3}$, where the attenuation constants a and x_0 are collected in table 1. This curve is referred to as the G-model on all plots.

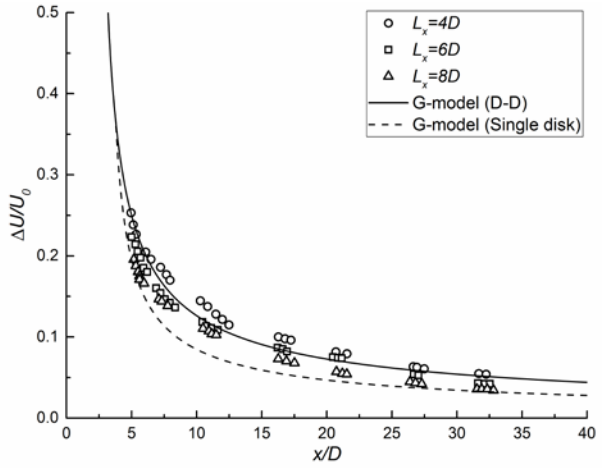

Figure 2. Development of the deficit velocity in the far wake behind the disk-disk configuration for different interspatial distances, L_x = 4, 6, 8*D*.

As seen from the graph of figure 2, the velocity deficit of the far wake from the disk-disk setup (D-D) is well described by the G-model. For clarity, the graph also displays the wake development for a single disk from [6]. The two data sets of figure 2 indicate the existence of similar growth rates with

the same exponent (-2/3) of the wake behind the dual system of the two passive disks as compared with the single disk. From this figure, it is possible to estimate the attenuation constants of the two wakes of the single disk and the passive D-D system (Table 1). Figure 2 also shows that the total wake deficit increases when the distance between the disks decreases from L_x = 8*D* to 4*D*. This is as expected, as the interaction between two passive bluff-bodies results in an increased deceleration as compared to a single wake.

Table 1. The attenuation constants for the single and dual configurations of the disk or rotor setups.

Type of the setup	*a*	x_0
Single disk	0.31	3.2
D-D (average)	0.49	2.1
Single rotor	0.85	3.2
R-R (optimal)	0.71	2.1

The other purpose of the investigation is to analyse the wake behavior behind two active wind turbine rotors (R-R) extracting power from the flow. To clarify the impact of wake interaction from two wind turbines, the development of rotor-rotor wake was investigated at different operating conditions by varying the TSR and the distance between the two rotors. The TSR for the first rotor (λ_1) was defined by the incoming freestream flow (U = 0.54 m/s) and the angular velocity of the servo drive n_1 = 2.29 rps. The TSR for the second rotor (λ_2) was calculated from the velocity in the wake of the first rotor, measured one diameter upstream of the second rotor. This data is presented in Table 2. Both rotors were operated at maximum power, which for the first rotor is at a TSR = 5. For the second rotor, the rotational speed was varied until optimum power conditions were achieved. From the table, the operational parameters of both rotors are shown.

Table 2. Correspondence between the tip speed ratio λ_1 and angular velocity n_1 of the first rotor and the determination of the incoming velocity, angular velocity n_2 and tip speed ratio λ_2 for the optimal operating regime of the second rotor.

Parameter	Values		
L_x - *distance*	4*D*	6*D*	8*D*
$\lambda_1 = 2\pi\, n_1 R/U_0$,	5	5	5
U_2/U_0	0.33	0.55	0.68
n_2, rps	1.51	2.01	2.18
$\lambda_2 = 2\pi\, n_2 R/U_2$	10	8	7

The thrust of the disk and rotor systems was measured in [11-12]. The ratio of the total thrust (C_{T2}+ C_{T1}) of the two dual systems to the single one (C_{T0}) was calculated by varying the distance L_x (Table 3).

Figure 3 shows experimental data of the velocity deficit in the wake of the rotor-rotor system for the optimal TSR of the two rotors (Table 2) and for different relative distances (L_x = 4, 6, 8*D*). As seen from the figure, the values decrease smoothly along the same G-curve, and with the attenuation constants of Table 1, for λ_1 = 5 and the optimal operational conditions λ_2 at the three R-R distances (Table 2).

Table 3. A ratio of the total trust coefficients of the dual systems (C_{T2}+ C_{T1}) to these values of the single cases C_{T0}

Type of the setup	*4D*	*6D*	*8D*
D-D	1.69	1.86	1.97
R-R (optimal)	1.32	1.65	1.74

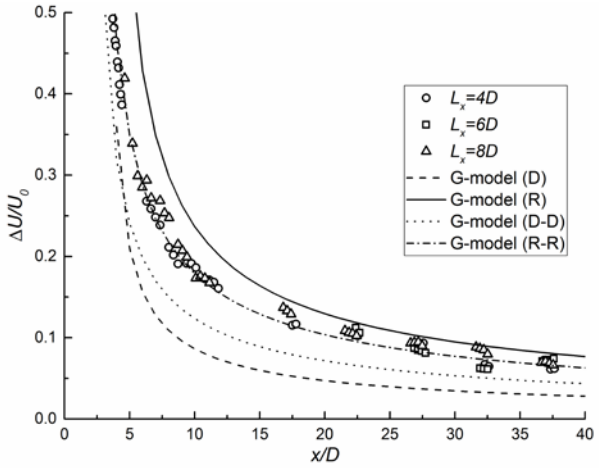

Figure 3. Development of the velocity deficit in the far wake behind the R-R system operating at optimal TSR for different interspatial distances, L_x = 4, 6 and 8*D*.

The comparison between the dual passive disks and the dual active rotors shows a strong difference between the wake behaviour of the two systems. The evaluation of both wake curves (figure 2) for the passive systems indicates an increase in the wake deficit behind dual disks (D-D), as compared to the single samples (D). In contrast to this (figure 3), the wake behind the active system of the dual rotors (R-R) decreases, as compared to the single samples (R). The last difference of the D-D and R-R systems indicates by the comparison of the total thrust in table 3. From this investigation, it is not clear why the duplication of the passive or active systems results differently in the wake deficit and thrust. One can just guess that a strong influence of the helical tip vortices producing the active systems only to explain these differences. Indeed, the helical vortex system behind rotors plays an important role in a generation of the velocity deficit in the wake. For example, these vortices can reduce the velocity in the near wake with up to two times as much as in the rotor plane, but the property has been studied for a single rotor only (see e.g. [7] and references hereby).

Another explanation for the difference between D-D and R-R systems may concern the differences in the resulting turbulence characteristics. Figure 4 shows a comparison of the distribution of the RMS-values in the wake behind all the considered disk and rotor systems.

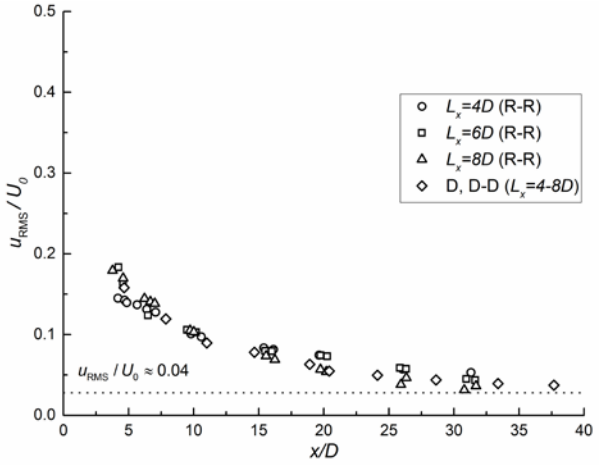

Figure 4. A comparison of RMS in the far wakes for both D-D and R-R systems.

As seen in the figure the distributions are almost equal. Hence, it can be concluded that it is not the turbulence characteristics that cause the different wake behavior of the different configurations. Thus, the most likely candidate for explaining the different behavior is that the tip vortex has an influence on

the wake characteristics in the rotor case that is not present when considering the flow about a disk. This will be the subject of a future study.

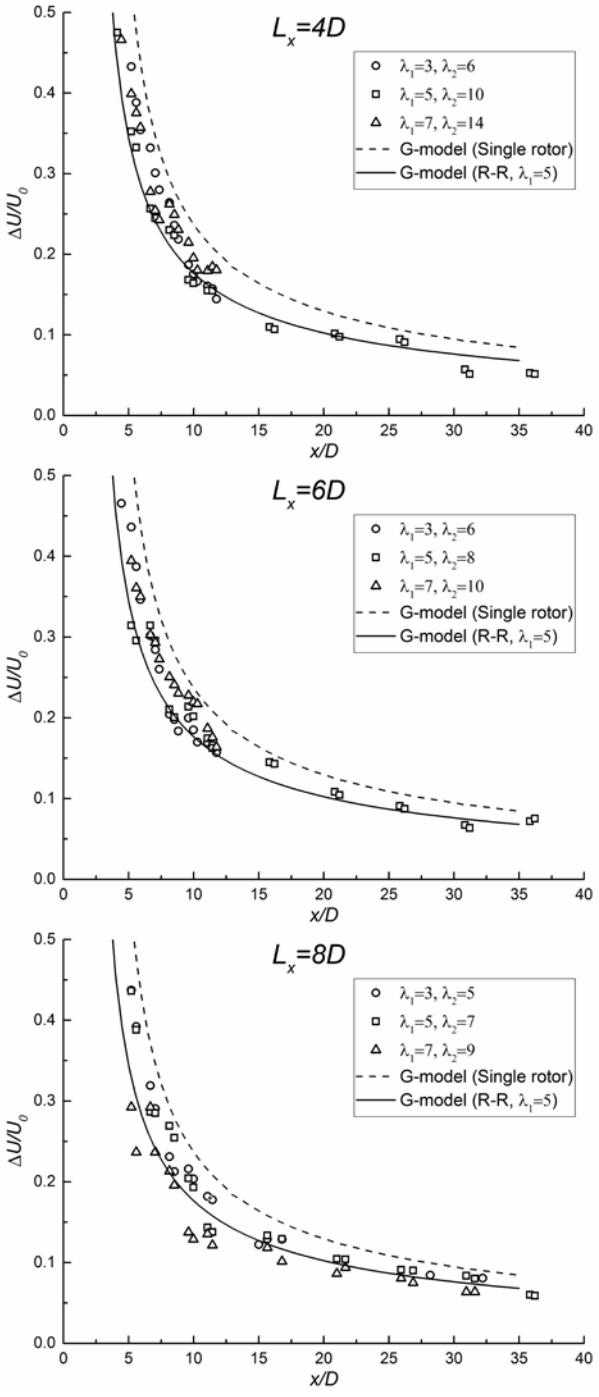

Figure 5. Development of the velocity deficit in the far wake behind rotor R-R systems operating at different TSR and different interspatial distances, L_x = 4, 6 and 8*D*.

Figure 5 shows the change in the maximum velocity deficit in the wake from a random sample of the R-R case varying both TSR and L_x. It is clearly seen that the velocity deficit decreases monotonically and in a smooth manner for all the considered cases without large deviation from the optimal regimes in Figure 3, shown by the solid line in Figure 5 (λ_1 = 5). Hence, we can conclude that

the variations of the operating regimes and rotor positions do not have a significant effect on the wake deficit in the far wake.

4. Conclusions

The far wake developments behind both disk-disk and rotor-rotor setups have been measured and analysed for different interspatial positions and operating regimes. The measurements show that the velocity deficits for all the considered cases follow a rational dependence with the same rate, but with different wake attenuation coefficients. Two main differences in the wake behavior for the disk-disk and the rotor-rotor systems were found. The resulting velocity deficit depends strongly on the distance between the dual disks and the wake intensity grows for the dual disks in comparison with the single one. In contrast to this, the decay of the velocity deficit behind dual rotors is nearly independent of the interspatial distance between the rotors and the wake intensity behind the dual rotor system is smaller than the one behind a single rotor. The differences may be explained by the influence of the rotor tip vortices which are absent in the disk-disk model. Thus, our experiments indicate that a dual disk system cannot satisfactorily replace a system of dual rotors when analysing wake properties behind wind turbines.

5. Acknowledgments

The research was supported by the Russian Science Foundation (Project № 14-19-00487) and the Danish Council for Strategic Research for the project Center for Computational Wind Turbine Aerodynamics and Atmospheric Turbulence (grant 2104-09-067216/DSF) (COMWIND: http://www.comwind.org).

References

[1] Vermeer L, Sørensen J, Crespo A. Wind turbine wake aerodynamics. *Prog. Aerosp. Science* 2003; 39: 467-510.
[2] Porte-Agel F,Wu YT, Chen CH. A numerical study of the effects of wind direction on turbine wakes and power losses in a large wind farm. *Energies*. 2013;6(10): 5297–5313.
[3] Okulov VL, Naumov IV, Mikkelsen RF, Sørensen JN, Wake effect on a uniform flow behind wind-turbine model *Journal of Physics Conference Series* 2015; 625: 012011.
[4] Naumov IV, Mikkelsen RF, Okulov VL. Estimation of Wake Propagation behind the Rotors of Wind-Powered Generators. *Thermal Engineering* 2016; 63(3): 208–213.
[5] Dufresne NP, Wosnik M. Velocity Deficit and Swirl in the Turbulent Wake of a Wind Turbine. *J. Marine Technology Society* 2013; 47(4): 193-205.
[6] Naumov IV, Litvinov IV, Mikkelsen RF, Okulov VL. Investigation of a wake decay behind a circular disk in a hydro channel at high Reynolds numbers. *Thermophysics and Aeromechanics* 2015; 22(6): 657-665.
[7] Naumov IV, Mikkelsen RF, Okulov VL, Sørensen JN. PIV and LDA measurements of the wake behind a wind turbine model. *Journal of Physics: Conference Series* 2014, 524: 012168; doi:10.1088/1742-6596/524/1/012168.
[8] Okulov VL, Naumov IV, Mikkelsen RF, Kabardin IK, Sørensen JN. A regular Strouhal number for large-scale instability in the far wake of a rotor. *J. Fluid Mech.* 2014; 747: 369-380.
[9] Selig M, Guglielmo J, Broeren A, Giguere P. Summary of Low-Speed Airfoil Data 1995; 1: 292.
[10] Okulov VL, Sørensen JN, Wood DH. The rotor theories by Professor Joukowsky: Vortex Theories. *Prog Aerospace Sci* 2015; 73: 19-46. DOI: 10.1016/j.paerosci.2014.10.002.
[11] Naumov I.V., Litvinov I.V., Mikkelsen R.F., Okulov V.L.Experimental investigation of wake evolution behind a couple of flat disks in the hydro channel. *Thermophysics and Aeromechanics* 2016; 23(5).
[12] Okulov V.L., Naumov I.V., Tsoy M.A., Mikkelsen R.F. Efficiency losses at coaxial arrangement of a pair of wind rotors. *Thermophysics and Aeromechanics*, 2016; 23(6).